Annals of Nuclear Energy 208 (2024) 110773

Contents lists available at ScienceDirect

Annals of Nuclear Energy

journal homepage: www.elsevier.com/locate/anucene

OFFBEAT V&V studies for REBEKA tests on cladding ballooning and burst during LOCA conditions

L. Verma [a,*], I. Clifford [a], P. Konarski [a], A. Scolaro [b], H. Ferroukhi [a]

[a] Paul Scherrer Institut (PSI), Laboratory for Reactor Physics and Thermal Hydraulics (LRT), Forschungsstrasse 111, 5232 Villigen PSI, Switzerland
[b] Ecole Polytechnique Fédérale de Lausanne, Laboratory for Reactor Physics and Systems Behaviour (LRS), 1005 Lausanne, Vaud, Switzerland

ARTICLE INFO

Keywords:
Fuel performance
OFFBEAT
LOCA
Ballooning
Validation

ABSTRACT

The OpenFOAM Fuel Behaviour Analysis Tool (OFFBEAT), developed jointly by EPFL and PSI in Switzerland, is rapidly gaining recognition as a comprehensive code for multi-dimensional thermo-mechanical fuel behaviour analysis. Like for any novel code, verification and validation (V&V) studies are crucial to test the capabilities of the code as new developments are made. The verification and validation of OFFBEAT is an ongoing effort and new verification studies are done as new models or methodology is implemented in the code. At the same time validation against experimental data are carried out to test the capabilities of the code to simulate fuel behaviour in normal and accidental conditions. In this paper, validation studies of OFFBEAT have been done for the REBEKA tests, which are separate effects tests to obtain data on cladding ballooning and burst under typical loss-of-coolant accident (LOCA) conditions. For the verification study, a code-to-code comparison of OFFBEAT is made with more validated codes such as Falcon and BISON. The results are compared with those obtained using Falcon, which is the reference fuel performance code at PSI, and with the results available in open literature using the BISON fuel performance code.

A 2D axisymmetric analysis has been done to predict the burst temperature as a function of the rod internal pressure at different heating rates. The obtained results are compared with experimental data and are found to be in good agreement. The code-to-code comparison with BISON and Falcon shows that OFFBEAT results are in close agreement to BISON results, whereas Falcon underpredicts the burst temperatures. Further 3D analysis has been done using OFFBEAT and the 3D results are in good agreement with the 2D results, showcasing OFFBEAT's capabilities to model multi-dimensional phenomena. An azimuthal temperature gradient in the cladding leads to non-uniformity in the ballooning of the cladding, bowing of the cladding and higher burst temperatures, which was also predicted in the experiments and in the study done using the BISON code.

This V&V study provides great insights into the cladding ballooning and burst behaviour in separate-effects tests during LOCA conditions and proves OFFBEAT's capability to simulate multi-dimensional, macroscopic fuel behaviour during accident scenarios.

1. Introduction

The nuclear fuel during irradiation experiences a variety of physical phenomena which impact its thermophysical, mechanical, and chemical properties. In order to carry out safe operations of nuclear reactors and for maintaining fuel rod integrity, it becomes imperative to have a thorough understanding of fuel behaviour for macroscopic phenomena occurring in the nuclear fuel. Understanding the behaviour of nuclear fuels relies on the development of fuel performance codes which are becoming more advance with the improved computational tools and high-performance computing. Well-known and highly developed fuel performance codes around the world include traditional codes such as TRANSURANUS (Lassmann, 1992), FRAPCON (Berna et al., 1997), FRAPTRAN (Geelhood et al., 2011) and Falcon (Rashid et al., 2004) as well as multi-dimensional codes like ALCYONE (Marelle et al., 2016) and BISON (Williamson et al., 2012). In order to test the capabilities and the accuracy of these fuel behaviour codes, verification and validation (V&V) studies need to be carried out. Examples of such V&V studies done using these popular codes, such as using BISON (Williamson et al., 2016), FRAPCON (Geelhood et al., 2011), and TRANSURANUS (Van

* Corresponding author.
E-mail address: lokesh.verma@psi.ch (L. Verma).

https://doi.org/10.1016/j.anucene.2024.110773
Received 12 June 2024; Received in revised form 1 July 2024; Accepted 5 July 2024
Available online 15 July 2024

Uffelen et al., 2008) are available in open literature. OFFBEAT (Scolaro et al., 2020) is a more recent multi-dimensional thermo-mechanical fuel performance code which is constantly evolving and developing in order to accommodate simulations of fuel behaviour phenomena, not only in normal operating conditions, but also during accident transients. The V&V of OFFBEAT goes hand-in-hand with the developments incorporated in the code. The set of initial validation database for OFFBEAT were presented in (Scolaro et al., 2022). More recently, the initial validation efforts for loss of coolant accident scenarios were presented in (Brunetto et al., 2023).

The accident conditions in a nuclear reactor can be design-basis accident (DBA), or beyond design-basis accident (BDBA). For a DBA, the plant design must ensure a core coolable configuration (Van Uffelen et al., 2010). One of the most important DBAs in the context of light water reactors is a loss-of-coolant accident (LOCA). A LOCA in a water-cooled reactor comprises a break in the coolant system leading to subsequent loss of core cooling capability. Despite fast shutdown of the reactor (SCRAM), the decay heat continues to be active and in absence of the coolant, the temperatures continue to rise. If a LOCA occurs, coolant depressurization can occur instantaneously, along with the increase in cladding temperature due to the deteriorating heat transfer caused by the loss of coolant. At some point the cladding diameter begins to increase and the cladding starts to deform locally. This local plastic deformation is known as cladding ballooning and can cause the cladding to burst. Several experimental studies have been carried out to study the effects of fuel rod behaviour during LOCA scenarios. These include separate-effects tests, focusing on the cladding behaviour without the complexities of fuel related behaviour, such as PURZY (Perez-Feró et al., 2010), REBEKA (Erbacher et al., 1982) (Markiewicz and Erbacher, 1988), QUENCH-L1 (Stuckert et al., 2018), as well as integral fuel rod tests, such as the ones in the Halden IFA-650 series (Wiesenack, 2013).

OFFBEAT has been upgraded to include simulation of LOCA scenarios. The implementation of a large-strain approach and the models for LOCA conditions were presented in Brunetto et al. (Brunetto et al., 2023). They also presented the initial validation efforts for the LOCA conditions in the PURZY (Perez-Feró et al., 2010) separate effect tests and for the IFA 650.2 (Ek, 2005) integral test. In this paper, the validation campaign for LOCA scenarios is extended by validating OFFBEAT against the REBEKA separate-effects tests (Erbacher et al., 1982) (Markiewicz and Erbacher, 1988) for cladding ballooning and burst. In doing so, the multi-dimensional capabilities of OFFBEAT are also showcased. Both 2D and 3D analyses have been done using OFFBEAT and the results are compared with those obtained from Falcon fuel performance code and with analyses available in open literature using the BISON fuel performance code. The multi-dimensional capabilities of OFFBEAT also enabled to analyze the effects of azimuthal temperature gradient on the cladding surface on the ballooning and burst characteristics. Initial results from the 2D and 3D analyses were presented in (Verma et al., 2024).

In the next section (section 2), OFFBEAT models and capabilities for LOCA simulations are presented in brief. The description of the REBEKA experiments and the validation study using OFFBEAT is presented for the 2D analysis in section 3. The results obtained with OFFBEAT are compared with Falcon and BISON results and presented in the following section 4. In section 5, the 3D analysis done using OFFBEAT and the effects of azimuthal temperature gradient are presented. Finally, the conclusions from the results are reported in section 6.

2. OFFBEAT capabilities for LOCA simulations

2.1. OFFBEAT fuel performance code

The OpenFOAM Fuel Behavior Analysis Tool, OFFBEAT (Scolaro et al., 2020) (Scolaro, 2021), is a multidimensional thermo-mechanical fuel performance code co-developed at the Ecole Polytechnique Fédérale de Lausanne (EPFL) and the Paul Scherrer Institut (PSI). As the name suggests, OFFBEAT uses OpenFOAM as development platform, which is an open-source C++ numerical library and uses the finite-volume-method (FVM) for the discretization and solution of the partial differential equations (PDEs). This is something which differentiates OFFBEAT from other fuel performance codes which typically use the finite-element-method (FEM) or the finite-difference-method (FDM) for the solution of the PDEs. OFFBEAT can be used for the transient analysis of complex 2D and 3D phenomena as well as for the 1.5D or 2D axisymmetric study of the steady-state base irradiation (Scolaro et al., 2020). OFFBEAT is also fully parallelized and the parallelization is achieved through geometrical domain decomposition. OFFBEAT utilizes a segregated solution scheme, in which the coupled neutro-chemical-thermo-mechanical behavior of a fuel rod is decomposed into simpler sub-sections, easier to solve (Scolaro et al., 2020). Two important components of OFFBEAT include a thermal sub-solver to calculate the temperature distribution and a mechanical sub-solver to calculate the deformation of the fuel rod. The thermal sub-solver deals with obtaining the temperature field by solving the heat diffusion equation, whereas the mechanical sub-solver deals with solving the three coupled momentum balance equations to obtain the displacement vector field. Other sub-solvers also included in OFFBEAT are an element transport sub-solver, neutronics sub-solver, and a recently developed flow sub-solver. Further details about OFFBEAT code, along with the models for fuel, cladding and gap behaviour and material properties can be found in the works of Scolaro et al. (Scolaro et al., 2020) (Scolaro, 2021).

2.2. Large-strain approach for large deformations

The mechanical solver in OFFBEAT deals with solving the linear momentum conservation equation to obtain the displacement and stress distributions. As the main applications of OFFBEAT focused mostly on base-irradiation conditions, where the deformations are significantly smaller than the characteristic dimensions of the body, the initial version of OFFBEAT incorporated the small-strain approximation for the mechanics solver (Scolaro et al., 2020). When large body rotations or deformations are involved, as are often encountered during accident transients like a LOCA, a large-strain approach is needed to investigate such considerable deformation. In order to simulate accidental transients, the mechanical framework of OFFBEAT has been extended to include the large-strain approach (Brunetto et al., 2023). Other fuel performance codes also include or have been extended to a large-strain formulation for analysis of accidental transients like LOCA. The most notable examples include the extension to large-strain of the TRANSURANUS code (Di Marcello et al., 2014), a mono-dimensional logarithmic strain framework in ALCYONE (Helfer, 2015), and the incorporation and validation of a large strain mechanical framework for LOCA tests in the BISON fuel performance code (Williamson et al., 2016).

In order to simulate LOCA scenarios, additional models for high temperature conditions are incorporated into OFFBEAT (Brunetto et al., 2023). Such high temperature conditions lead to specific phenomena which are rather insignificant or non-existent during normal standard temperature operations, such as cladding ballooning and burst. Some of these models include a dedicated cladding thermal creep model for high-temperature regime, a Zirconium β-phase transition model, and a burst failure criterion. During normal operating conditions, the Limbäck and Anderson (Limbäck and Andersson, 1996) model is used as the Zircaloy cladding creep model in OFFBEAT. For high temperature conditions, as those reached in LOCA scenarios, the creep model correlations are dictated by three different temperature regimes. For temperatures, $T < 700$ K, the normal standard operating regime is considered and the Limbäck and Anderson (Limbäck and Andersson, 1996) model is used. For temperatures, $T > 900$ K, the high temperature regime is considered and the Erbacher creep model (Erbacher et al., 1982) is used. A transitional regime is considered for temperatures in the intermediate range, $700 < T < 900$ K, wherein a logarithmic interpolation between the standard and high temperature creep strain rates is made.

The crystallographic phase transition of Zircaloy from α-phase at room temperature to a more stable β-phase at higher temperatures (above 1000–1100 K) also becomes important during LOCA conditions as it impacts the thermal creep rate, enhancing it significantly. A dynamic β-phase transition model based on the model by Massih (Massih, 2009) has been incorporated in OFFBEAT to account for the kinetics of the phase transformation.

To determine the moment the cladding failure due to burst during LOCA has occurred, simplified failure criteria are defined. The ones currently available in OFFBEAT are: (i) an overstrain criterion, in which the cladding is considered to have failed due to burst if the hoop creep strain exceeds a limiting value of hoop creep strain provided as input. A default value of 40 % engineering strain is used in OFFBEAT, (ii) an overstress criterion, in which the cladding is considered to have failed if the hoop stress exceeds a limiting value of burst stress. The burst stress correlation also depends on the oxidation parameters, but the contribution of oxidation is not yet implemented in OFFBEAT, (iii) a plastic instability criterion, in which the cladding is considered as failed if the effective plastic (creep + plasticity) strain rate reaches a limiting value of 100 $h^{-1} \approx 2.78x10^{-2}$ s^{-1}, (iv) a combined failure criterion, in which cladding fails when either of the two criteria selected are fulfilled. The limiting values used for the overstrain and the plastic instability criteria are based on the large strain mechanical solver in TRANSURANUS (Di Marcello et al., 2014).

3. Validation study for REBEKA tests

As mentioned already, the validation campaign of OFFBEAT against experiments is an ongoing effort. Several validation cases have previously been carried out to compare the results obtained by OFFBEAT for some key parameters with experimental data. The initial OFFBEAT validation cases focused on comparing integral parameter values like the fuel centerline temperature (FCT) and the fission gas release (FGR) (Scolaro et al., 2022) (Scolaro, 2021). More recently, with the incorporation of the large-strains approach, the validation campaign was extended to compare more complex phenomena like cladding ballooning and burst (Brunetto et al., 2023) with experiments. As an extension to this validation matrix, OFFBEAT has been validated against the REBEKA tests for cladding ballooning and burst during LOCA conditions.

3.1. REBEKA experiment description

The **RE**actor typical **B**undle **E**xperiment **Kar**lsruhe, REBEKA, separate-effects tests (Erbacher et al., 1982) (Markiewicz and Erbacher, 1988) are temperature transient tests in steam performed on single Zircaloy-4 cladding tubes used in PWRs at a variety of rod internal pressures and heating rates. The experiments were carried out in the REBEKA single rod test equipment of Kernforschungszentrum Karlsruhe (KfK) in the IRB institute in Karlsruhe. The purpose of the tests was to analyze the cladding behaviour and obtain data of cladding ballooning and burst when subjected to LOCA conditions.

The cladding tubes were heated from the inner side by an electrically insulated heater rod. In order to replicate the fuel, a stack of Al_2O_3 annular pellets surrounding the heater rod was used. The tubes had a heated length of 325 mm with inner diameter of 9.30 mm and outer diameter of 10.75 mm. The internal rod pressure was varied in a range of 1 to 140 bar for heating rates of ≈ 1 to 35 K/s. The surrounding test atmosphere was stagnant steam at atmospheric pressure and at a temperature of 473 K. The uniform temperature at the cladding circumference was maintained by heating with a shroud heater tube. Thermocouples spot-welded on the outer surface of the cladding were used to measure the cladding temperatures. For the tests on azimuthal temperature gradients, the shroud heater was switched off, generating a temperature difference around the cladding. The test section of the single rod test in REBEKA experiments is presented in Fig. 1(a). The information about the properties of the cladding tube can be found in the technical report KfK4343 (Markiewicz and Erbacher, 1988) and additional information can be found in (Erbacher et al., 1982). The burst temperature variation with rod internal overpressure at different heating rates from the REBEKA test is shown in Fig. 1(b). It was noted that with the same heating rate, a higher rod internal overpressure results in a lower burst temperature and a higher heating rate leads to higher burst temperatures for the same rod internal pressure (Erbacher et al., 1982).

3.2. 2D analysis using OFFBEAT

The OFFBEAT geometry used for the analysis consisted only of the cladding tube. For the 2D analyses, only the lower half of the heating rod was simulated, considering symmetric boundary conditions on the cladding top surface and a zero-displacement boundary condition on the cladding bottom surface. The presence of the internal heater was simulated by assuming a time-dependent temperature boundary condition on the cladding inner surface. Since the heater provides a uniform axial temperature, in order to replicate the power generation from the fuel, a simple linear axial temperature variation from the bottom to the top of the heating rod, peaking at the tube mid-plane was assumed. As in the experiments, the cladding was equilibrated initially at room temperature before the temperature ramp. The initial cladding temperature profile is shown in Fig. 2 along with the cladding tube to represent the axial variation, peaking at tube mid-plane. Different cases with case-specific rod internal pressure values were provided as pressure boundary condition on the cladding inner surface, while the cladding outer surface was provided with a fixed pressure of 1 atm.

A total of 20 cases with rod internal pressures in the range of 1–14 MPa, and three heating rates of 1, 10 and 30 K/s were carried out. The incremental large-strain solver with mesh update at the end of each time-step was used as the mechanical solver. The creep model used is based on Limbäck and Anderson model (Limbäck and Andersson, 1996) for the standard temperature region and the Erbacher model (Erbacher et al., 1982) for the high temperature region. The overstrain criterion was adopted as the failure criterion with the hoop strain limit set at 33.6 % true strain, which is equivalent to 40 % engineering strain. Most of the simulation setup along with the hoop strain limit was consistent with a previous validation study of the REBEKA test done using BISON fuel performance code by Pastore et al. (Pastore et al., 2021). Doing so provides an opportunity for OFFBEAT results to be compared with an existing validation study by BISON and to test how close or different the results obtained from the two codes are. This code-to-code comparison with BISON as well as with Falcon code is presented later in the paper.

3.2.1. OFFBEAT simulation and results

A 2D axisymmetric model was adopted in OFFBEAT with 10 and 80 cells in the radial and axial directions, respectively. The simulation was set to stop as soon as the failure criterion was met. Each of the 20 cases led to failure of the cladding and the respective burst temperatures and time of burst were obtained. Fig. 3 shows the plot for burst temperatures at different rod internal pressures and heating rates. The scatter points for the experimental data were digitized using WebPlotDigitizer (Rohatgi) from the original experiment plot in Fig. 1(b).

The expected trend of decreasing burst temperatures with increasing rod internal pressures is evident from the results. Also, the burst temperature for the same rod pressure increases with increasing heating rates. The results obtained by OFFBEAT are found to be in good agreement with the experimental data with a slight underprediction for the heating rate of 1 K/s. The results are found to be closer to the experimental data at lower internal pressure and higher heating rates. The time of burst and the burst temperatures for each of these cases are

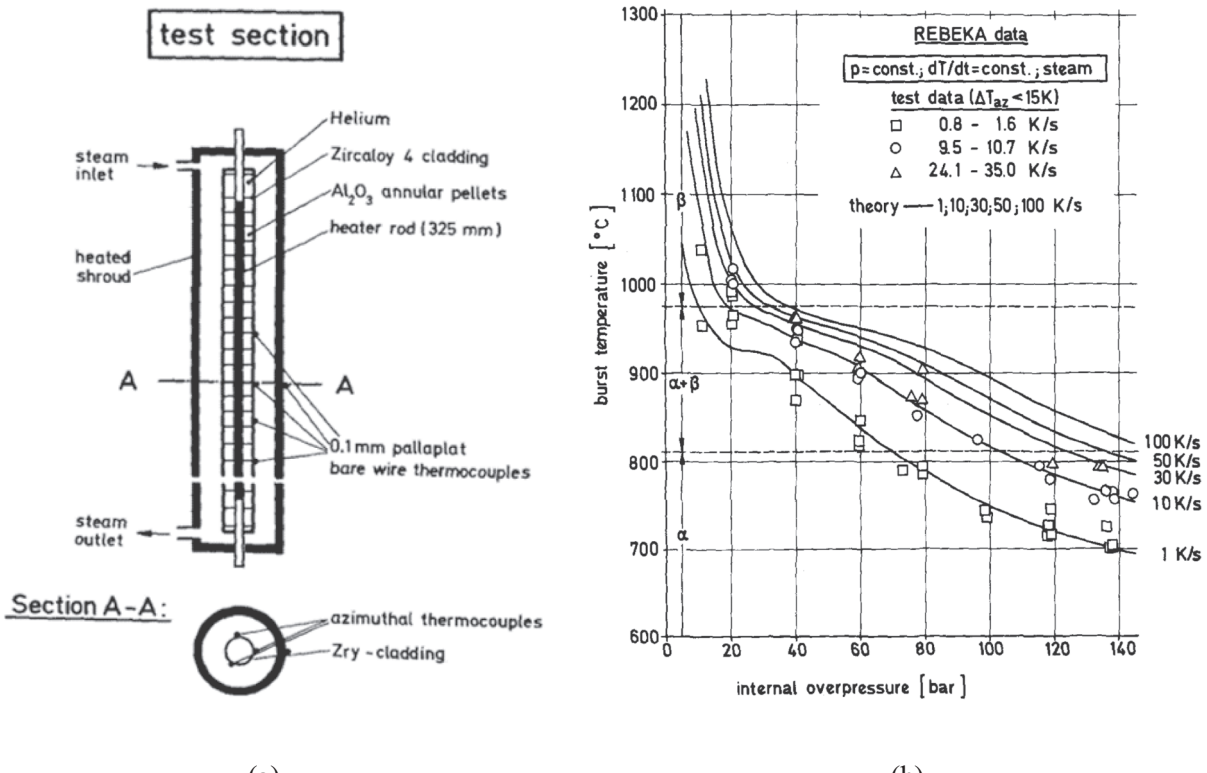

Fig. 1. (a) The test section of the single rod test, (b) burst temperature vs internal overpressure of Zircaloy claddings at different heating rates (From (Erbacher et al., 1982)).

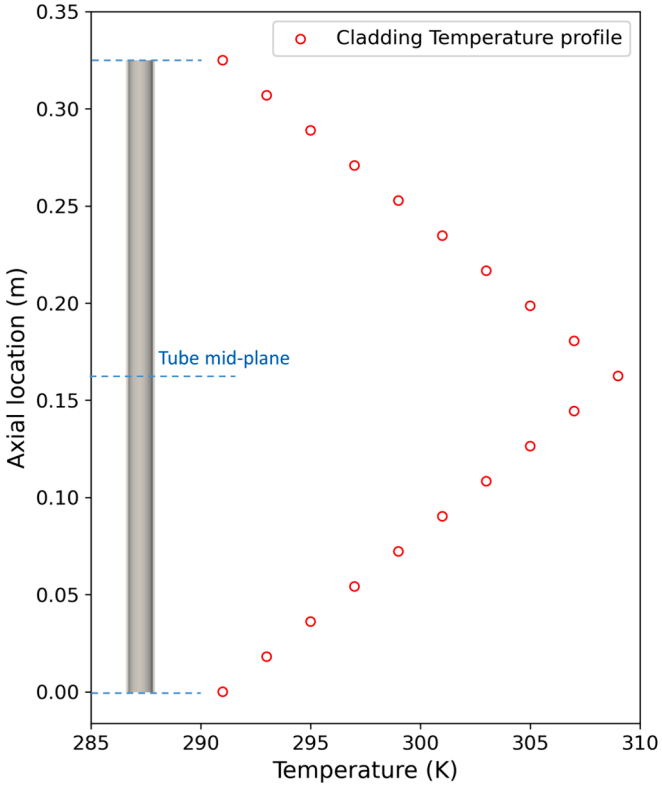

Fig. 2. Assumed initial time-dependent temperature boundary condition on the cladding inner surface.

presented in Table 1. As is evident, for the same heating rate, with higher internal rod pressures, the failure occurs earlier and thus the temperatures reached at burst are lower.

For the particular case with rod internal pressure 10 MPa and heating rate of 1 K/s, the contours for temperature and hoop creep strain at the time of burst are shown in Fig. 4. The visualizations were created using ParaView 5.9.1 visualization tool (Ahrens et al., 2005). The lower half of the tube is reflected on the z-axis to get the full view and the displacement is scaled by a factor of 4 in the radial (x-axis) for better visualization. The cladding ballooning is evident at the tube mid-plane where the creep strain is maximum and where the burst occurs. The temperature at burst is found to be 1002.4 K with the hoop creep strain reaching the failure limit of 33.6 % for the true strain.

The time evolution of hoop creep strain for this case is presented in Fig. 5(a). It can be noticed that the burst (hoop creep strain = 33.6 %) occurred at 693.54 s, with strain increasing from 20 % to the point of burst within ≈4 s (as seen from the faded region in the figure). The same plot with the log scale for the y-axis is shown in the inset. This trend can be better understood by observing the effects of the different creep models in OFFBEAT as presented in Fig. 5(b), which plots the same log scale hoop creep strain as a function of temperature. As mentioned earlier, OFFBEAT uses the Limbäck and Anderson creep model for temperatures $T < 700$ K, the Erbacher creep model for $T > 900$ K and an interpolation from the two in the range $700 < T < 900$ K. No significant hoop creep strain is observed in the standard temperature region up to 700 K, at which point the creep model switches from the Limbäck and Andersson model to the interpolation regime. At 900 K, the Erbacher creep model is activated, and the hoop creep strain values start to increase rapidly, reaching the hoop creep strain limit of 33.6 % within the next 100 s, with the temperature at burst reaching 1002.4 K.

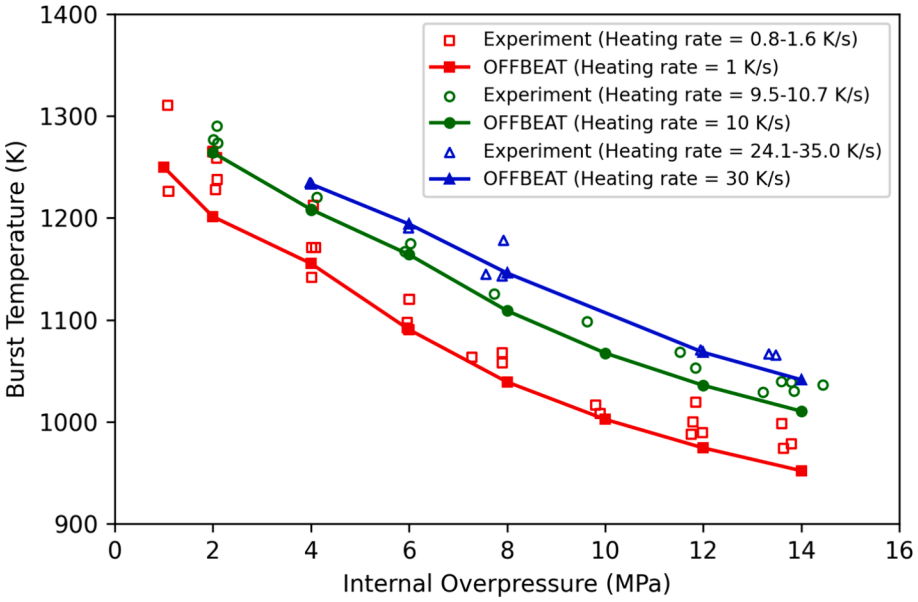

Fig. 3. Comparison of OFFBEAT results against experiment data for burst temperature vs internal rod pressure for pressure in the range of 1–14 MPa and heating rates of 1, 10 and 30 K/s.

Table 1
Burst temperatures and time of burst at different pressures and heating rates.

Pressure (MPa)	Heating rate 1 K/s		Heating rate 10 K/s		Heating rate 30 K/s	
	Burst Temperature (K)	Time of burst (s)	Burst Temperature (K)	Time of burst (s)	Burst Temperature (K)	Time of burst (s)
1	1249.88	940.994	–	–	–	–
2	1201.31	892.425	1264.25	95.536	–	–
4	1155.32	846.437	1208.40	89.952	1233.33	30.815
6	1090.52	781.636	1164.10	85.521	1194.07	29.506
8	1039.08	730.191	1108.98	80.010	1145.96	27.902
10	1002.43	693.543	1067.47	75.858	–	–
12	974.398	665.511	1035.79	72.690	1068.17	25.309
14	952.021	643.135	1010.45	70.1559	1041.28	24.413

3.2.2. Effect of different strain definitions

The large strain analysis also requires a consistent formulation of the strain tensor. Several strain tensor definitions are implemented in OFFBEAT, and the strain–displacement relation can be defined in several ways. It becomes imperative to check how using the different definitions can impact the results obtained. The most common definition is the engineering strain which is defined as the ratio of total deformation to the initial dimension of the material body on which forces are applied:

$$e = \frac{l - L}{L} \tag{1}$$

where e is the engineering strain, l is the final length and L is the original length. For our analysis, we consider a failure limit on the engineering strain at 40 %. Other definitions of strain that are available to choose from in OFFBEAT are presented below in relation to the engineering strain:

- **Logarithmic strain** (or Hencky or true strain), which can be defined as:

$$\delta\varepsilon_l = \frac{\delta l}{l} \tag{2}$$

where ε_l is the logarithmic strain and it can be integrated and then expressed in terms of the engineering strain, e, as:

$$\varepsilon_l = \ln(1 + e) \tag{3}$$

Here, $e = 0.40$ would be equivalent to $\varepsilon_l = 0.33647$, which means 33.64 %. We have used the logarithmic strain definition for our 2D analysis presented earlier.

- **Euler-Almansi strain**, ε_E, which can be defined as:

$$\varepsilon_E = \frac{1}{2}\left(\frac{l^2 - L^2}{l^2}\right) = \frac{1}{2(e+1)^2}\left[e^2 + 2e\right] \tag{4}$$

Here, $e = 0.40$ would be equivalent to $\varepsilon_E = 0.24489$, which means 22.45 %.

- **Green-Lagrange strain**, ε_G, which is defined as:

$$\varepsilon_G = \frac{1}{2}\left(\frac{l^2 - L^2}{L^2}\right) = \frac{1}{2}\left[e^2 + 2e\right] \tag{5}$$

Here, $e = 0.40$ would be equivalent to $\varepsilon_G = 0.48$, which means 48 %.

Using these different definitions of strains, a sensitivity analysis is carried out for the same 2D analysis for the case with 8 pressure values and a heating rate of 1 K/s. The plot for burst temperature vs internal overpressure for the different strain definitions is presented in Fig. 6. It is noticed that the results obtained using the different strain definitions are very similar to each other and in good agreement to the experimental data.

A magnified view of the burst temperature values at pressure 10 MPa obtained using the three definitions is also shown in the figure. A maximum difference of 2 K is noted among the three observations. From

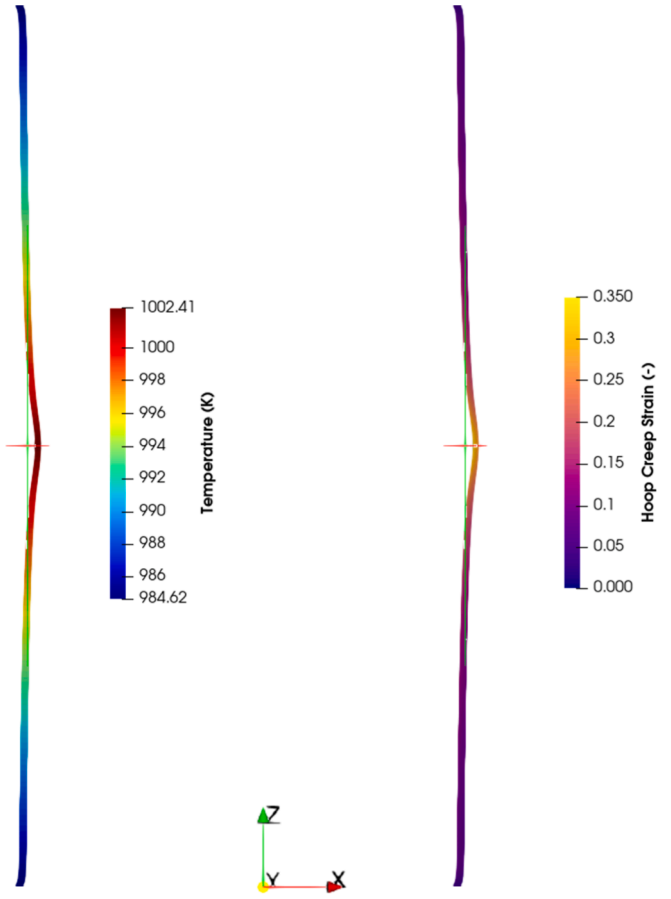

Fig. 4. Contours of cladding tube burst temperature and hoop creep strain for the case with P = 10 MPa and heating rate = 1 K/s.

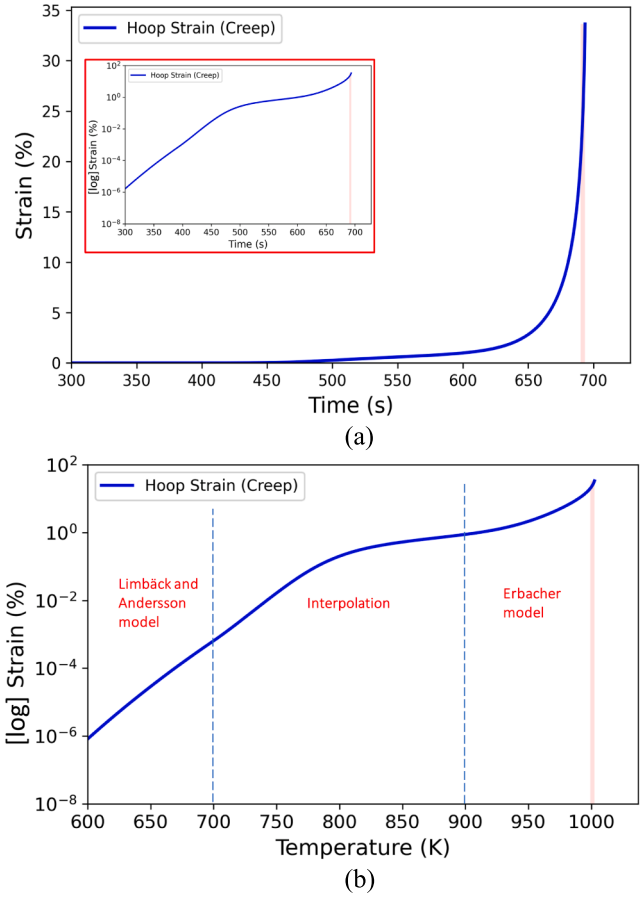

Fig. 5. (a) Time evolution of hoop creep strain (b) hoop creep strain (log scale) vs temperature.

this sensitivity analysis, it is concluded that the different strain definitions do not impact the result if the correct equivalent limit for the failure criterion is used. This conclusion is corroborated by the fact that, as seen in Fig. 5, the strain values increase from 20 % to burst limit values within ≈4 s with a rise in temperature of only 4 K. For the definitions presented here, the hoop creep strain limits are within the range 20–50 %, and thus, failure occurs within seconds form each other in each of these cases, leading to similar burst characteristics.

4. Verification of results against other codes

In order to test how OFFBEAT results compare with other fuel performance codes, a code-to-code comparison study was carried out. A study for the REBEKA tests carried out using BISON fuel performance code by Pastore et al. (Pastore et al., 2021) is available in open literature. Additionally, the 2D analysis done with OFFBEAT was also carried out using the Falcon fuel performance code. A small description for the two codes along with the simulation conditions and setup used for the analysis is presented below.

4.1. BISON

BISON (Williamson et al., 2012) is a modern parallel, FEM-based fuel performance code developed at Idaho National Laboratory (INL). The code can be used to study steady state as well as transient fuel behaviour for multi-dimensional geometries. BISON is built upon INL's Multi-physics Object-Oriented Simulation Environment (MOOSE) (Gaston et al., 2009) which is a parallel, finite element-based framework to solve systems of coupled non-linear partial differential equations.

The validation study for the REBEKA test using BIOSN was done by Pastore et al. (Pastore et al., 2021). The cladding models required to simulate LOCA conditions were implemented in BISON. These included a high temperature steam oxidation model, crystallographic phase transition model, high temperature creep model, and burst criteria models. In (Pastore et al., 2021), only the cladding was simulated, with the presence of the alumina pellets and the internal electric heaters being simulated using a time dependent Dirichlet temperature boundary condition on the cladding inner surface. For the pressure boundary conditions, constant case-specific pressure was provided to the cladding inner surface, with atmospheric pressure on the outer surface. A 2D axisymmetric geometry of only the lower half of the heated cladding length was modelled. The combined overstress and overstrain failure criterion were used to determine the cladding burst.

4.2. Falcon

Falcon (Rashid et al., 2004) is a 2D fuel behaviour code developed by EPRI and has been verified and validated to a great extent over the course of its development and usage. Falcon supports 2D axisymmetric analysis (r-z) of full-length fuel rods and can also be used for further detailed analysis of 2D slices (r-θ) at selected axial locations to study radial and angular effects. Based on a robust finite element numerical structure, Falcon is capable of analyzing both steady state and transient fuel behavior with a seamless transition between the two modes.

For the REBEKA validation study using Falcon, a 2D axisymmetric r-z geometry was used. Unlike OFFBEAT, the full heating length of 325 mm was simulated. It was mandatory to physically model the fuel in Falcon, so a fuel element with zero power was modelled, however, a large gap of

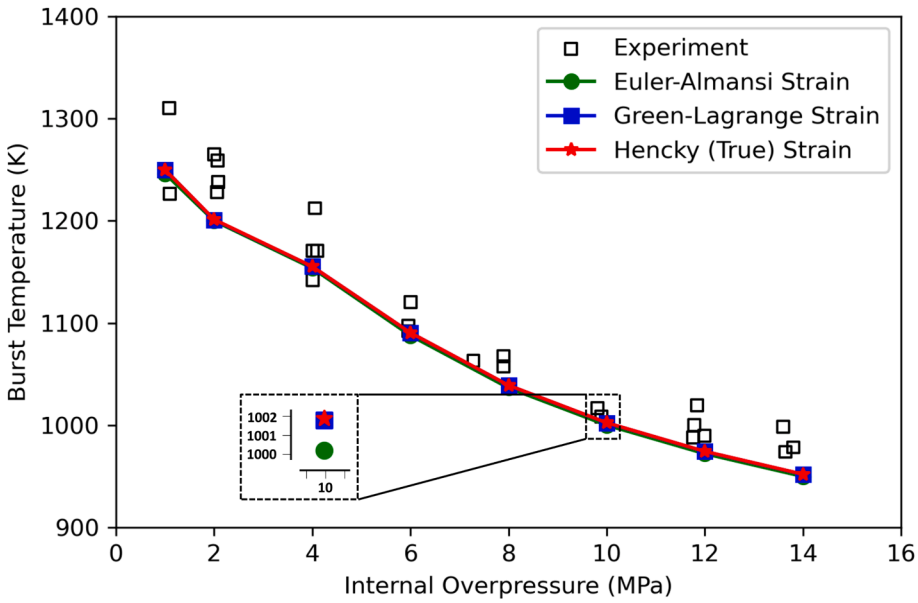

Fig. 6. Burst temperature vs internal overpressure for different strain definitions.

2.65 mm was considered to negate any influence of the fuel on the cladding. The cladding surface was provided with the same axial temperature profile as in OFFBEAT. The cladding was discretized into 2 radial stations and 11 axial stations. A finer mesh was also tested but it did not affect the results. The cladding creep model for the high temperature regime in Falcon is different from that in OFFBEAT. In Falcon, the Limbäck and Anderson creep model is used for the standard temperature regime (same as in OFFBEAT) and the MATPRO creep model (Hagrman and Reyman, 1979) in the high temperature regime. The transition temperature between the two regimes is set at 750 K. There is no option to set the failure criterion or limit in Falcon but the simulation crashes as soon as the cladding fails and the properties at burst can be determined.

4.3. Comparison results

Just like the OFFBEAT 2D analysis, 20 cases with rod internal pressure values in the range of 1–14 MPa and heating rates of 1, 10 and 30 K/s were used. The BISON results for these 20 cases were digitized using WebPlotDigitizer (Rohatgi) from Pastore et al. (Pastore et al., 2021). The Falcon simulations were carried out for these 20 cases using the same conditions as in the OFFBEAT analysis. The burst temperature vs internal pressure plots for OFFBEAT, BISON and Falcon for each heating rate of 1, 10 and 30 K/s are presented in Fig. 7(a), (b), and (c), respectively.

The general trend of decreasing burst temperature with increasing internal pressure as well as increasing burst temperature with increasing heating rates is followed in all the three codes. Between OFFBEAT and BISON, the results are comparably in good agreement with each other for all the cases. This is expected since the LOCA creep models used in these codes are consistent. OFFBEAT results tend to be closer to experimental data in all the cases than BISON, especially for the lower pressure values of 1 and 2 MPa for the heating rate of 1 K/s (Fig. 7(a)), where BISON results deviate from experiments, whereas OFFBEAT results still remain relatively close to experiments. According to Pastore et al. (Pastore et al., 2021), the discrepancies in their results could be due to the uncertainties inherent in the cladding creep, oxidation and phase transformation models, and 3D effects which cannot be captured in the 2D representation. The difference in the OFFBEAT and BISON results could be due to the difference in the axial temperature profile provided at the cladding inner surface. In OFFBEAT, a temperature difference of 9 K was considered in the temperature profile from the tube mid-plane to the bottom of the tube.

The results from Falcon are significantly underpredicted in all the cases. The results closest to the other two codes as well as to experiments are for heating rate 1 K/s (Fig. 7(a)), where in contrast to general observation, the burst temperatures are higher than in OFFBEAT and BISON for pressure of 1 MPa. The burst temperature and time of burst calculated using Falcon and OFFBEAT for all the 20 cases are presented in Table 2. We notice that for this particular case (red in the table), the burst temperature and also the time of burst are higher in Falcon, whereas they remain lower than OFFBEAT values for all the other cases. This shows that, apart from this exception, the burst occurs earlier in Falcon in comparison to OFFBEAT.

In order to better understand the difference in the results between Falcon and OFFBEAT, we focus on a particular case with pressure 10 MPa and heating rate 1 K/s. We find that for OFFBEAT, the burst occurs at the point when the hoop creep strain limit, which is set at 48 %, is reached. The Green-Lagrange strain definition was used for the OFFBEAT vs Falcon comparisons to be consistent with Falcon, which has only the Green-Lagrange strain definition available. This is why the hoop creep strain limit for the failure criterion was set at 48 %, although as shown earlier, the strain definition does not affect the results obtained in OFFBEAT. The temperature at burst for this case was 1002.4 K and the time of burst was 693.54 s. On the other hand, for Falcon, moments before the point of failure the hoop creep strain was 35.52 %. The temperature at burst was 951.89 K and the time of burst was 642.90 s. At the very next step the Falcon simulation crashed. The time evolution of the hoop creep strain in Falcon and OFFBEAT is plotted in Fig. 8(a). It is found that the hoop creep strains have similar trends, with low creep strain values and then very high values in a short span of time leading to burst. The apparent difference that can be noted from the figure is that the rise in hoop creep strain starts earlier in Falcon and thus, the cladding fails earlier, reaching lower burst temperatures than in OFFBEAT.

Also, in Fig. 8(b) the hoop creep strain is plotted against temperature for the two codes. The effect of the different high temperature creep models used in the two codes can be noticed. The dashed lines represent the transition temperatures for the creep models in OFFBEAT (blue) and Falcon (orange). The MATPRO high temperature creep model is activated in Falcon at 750 K, however, no significant rise in hoop creep

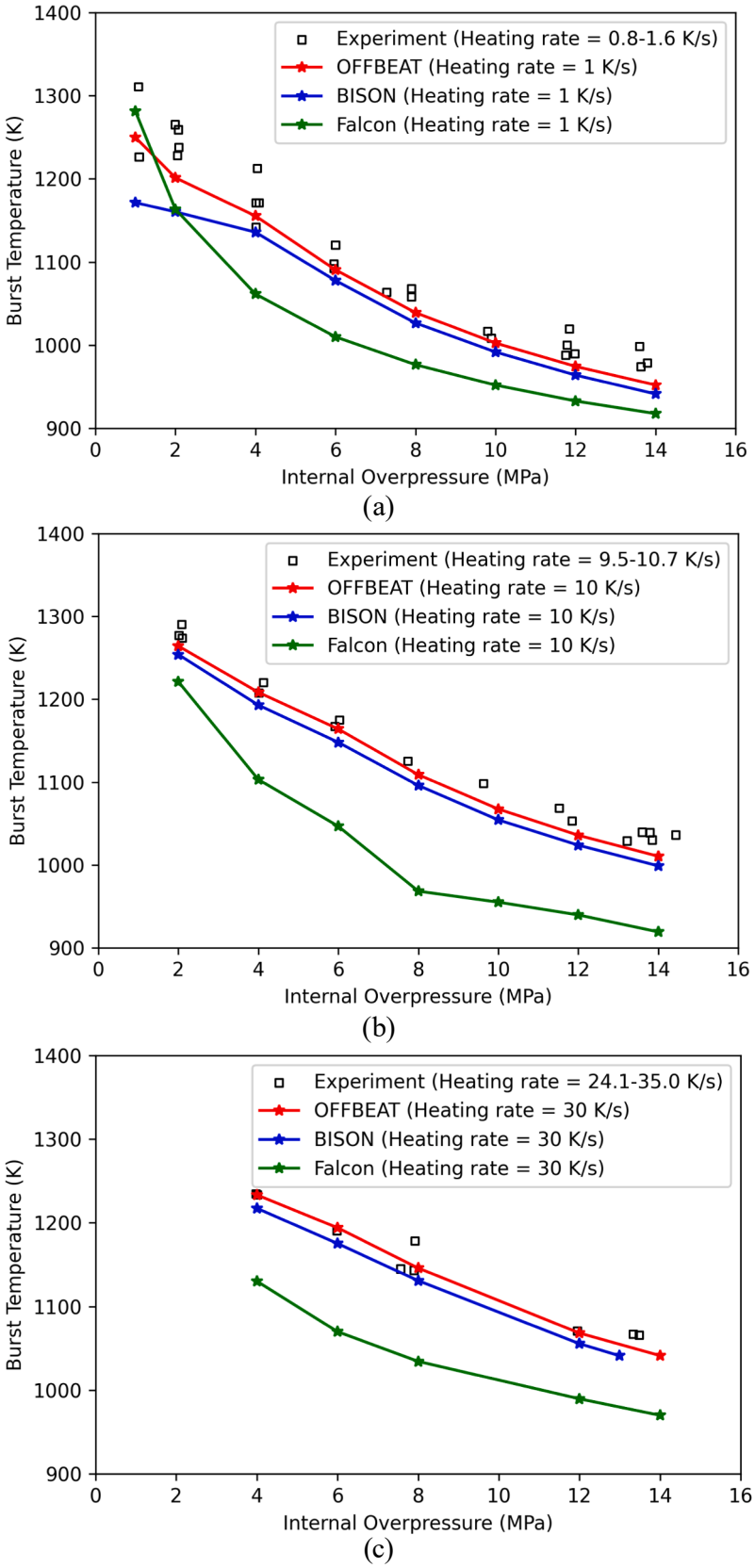

Fig. 7. Burst temperature vs internal pressure for OFFBEAT, BISON and Falcon for heating rate (a) 1 K/s, (b) 10 K/s and (c) 30 K/s.

Table 2
Comparison of Falcon and OFFBEAT burst temperatures and time of burst. (Red line denotes the only case where Falcon burst temperature and time of burst are higher than in OFFBEAT).

Heating rate 1 K/s				
Pressure (MPa)	Burst Temperature (K)		Time of burst (s)	
	OFFBEAT	Falcon	OFFBEAT	Falcon
1	1249.88	1281.115	940.994	972.121
2	1201.31	1163.342	892.437	854.347
4	1155.32	1061.454	846.437	752.458
6	1090.52	1009.893	781.636	700.898
8	1039.08	976.439	730.191	667.445
10	1002.43	951.891	693.543	642.896
12	974.39	932.756	665.511	623.761
14	952.02	917.597	643.135	608.602
Heating rate 10 K/s				
Pressure (MPa)	Burst Temperature (K)		Time of burst (s)	
	OFFBEAT	Falcon	OFFBEAT	Falcon
2	1264.25	1221.26	95.536	91.335
4	1208.40	1103.03	89.952	79.512
6	1164.10	1046.64	85.521	73.873
8	1108.98	968.35	80.010	66.044
10	1067.47	955.09	75.858	64.718
12	1035.79	939.69	72.690	63.178
14	1010.45	919.27	70.1559	61.136
Heating rate 30 K/s				
Pressure (MPa)	Burst Temperature (K)		Time of burst (s)	
	OFFBEAT	Falcon	OFFBEAT	Falcon
4	1233.33	1130.11	30.815	27.407
6	1194.07	1069.84	29.506	25.398
8	1145.96	1034.38	27.902	24.216
12	1068.17	989.59	25.309	22.723
14	1041.28	969.93	24.413	22.067

strain values is noticed up to around 900 K, after which the exponential rise in hoop creep values is observed leading to burst within the next 50 s with temperature at burst as 951.89 K. For OFFBEAT the burst takes around 100 s to occur after the high temperature creep model is activated at 900 K. This confirms Falcon's usage of a conservative creep model for LOCA. From the analysis, it seems that the different creep models for the high and intermediate temperature regimes used in Falcon and OFFBEAT lead to differences in the burst properties.

5. 3D analysis using OFFBEAT

With the multi-dimensional capabilities of OFFBEAT, further 3D analysis of the cladding ballooning and burst can be done using the data from the REBEKA test series. The case with internal rod pressure of 10 MPa and heating rate of 1 K/s is considered for the 3D analysis.

5.1. Simulation setup and results

For the 3D analysis, the geometry creation and meshing are done using the Coreform Cubit v2022.11 tool (Cubit, 2022) and upper half of the cladding tube is modelled and meshed. The meshed geometry has a total of 82′800 cells with (15 x 92 x 60) radial, axial and azimuthal cells, respectively. The upper half of the cladding tube geometry used for the 3D analysis is presented in Fig. 9.

The same boundary conditions as in the 2D case are applied with an axial temperature profile and fixed pressure of 10 MPa on the cladding inner surface and a fixed pressure of 1 atm on the cladding outer surface, symmetric boundary condition on the cladding bottom surface and a zero-displacement boundary condition on the cladding top surface. Considering the results from the 2D analysis, the limit for the hoop creep strain was set at 40 % and the 3D simulation was allowed to run even after the failure criterion was met. The OFFBEAT was run in parallel using 16 processors. The failure criterion was reached at t = 692.8 s and the simulation crashed within the next few time steps. The total time taken for the simulation was ≈ 2.5 h. The contour for the temperature at the time of burst is presented in Fig. 10. On the left the entire length of the cladding tube is presented, by mirroring the top half modelled tube along the z-axis. On the right is a magnified view of the cladding tube near the mid-tube region. The view has been sliced in the y-z plane to visualize the effects at the inner surface of the tube. There is no significant deformation of the cladding along the axial length of the tube, except near the tube mid-plane, where cladding ballooning occurs. In the figure, the cladding ballooning in the tube mid-plane region is clearly visible. The temperature at burst was found to be 1001.69 K. Further, similar contour plot for the hoop creep strain at the time of burst is presented in Fig. 11. It can be seen that the cladding reaches maximum hoop creep strain values near the tube mid-plane.

The hoop creep strain (in log scale) as a function of time and temperature is plotted in Fig. 12 and a similar behaviour to the 2D analysis can be noticed. As stated before, the time of burst for the 3D analysis was found to be 692.8 s with the burst temperature of 1000.69 K. As in the 2D analysis, the hoop creep strain was rather insignificant in the normal and intermediate temperature range with increase in values in the high temperature range leading to burst condition from 20 % strain within a few seconds.

The 3D analysis using OFFBEAT showed good agreement with the 2D analysis (Table 3) and demonstrated the multi-dimensional modelling capabilities of OFFBEAT for LOCA scenarios.

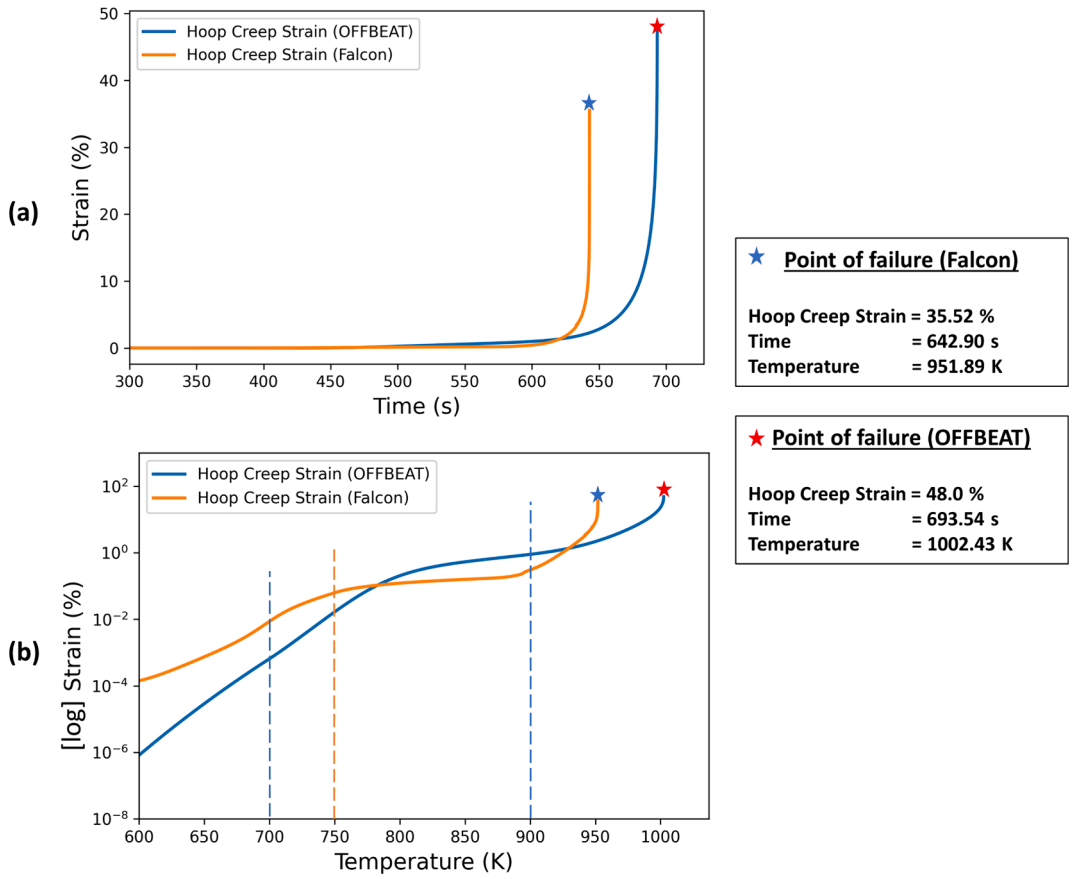

Fig. 8. (a) Time evolution of hoop creep strain (b) hoop creep strain (log scale) vs temperature, for Falcon and OFFBEAT simulations for P = 10 MPa and heating rate 1 K/s.

5.2. *Effect of azimuthal temperature gradient*

With the 3D analysis giving promising results, another study to analyze the effects of azimuthal temperature variation on the cladding tube is carried out. As mentioned earlier, in the REBEKA experiments, these tests were done by switching off the shroud heater which was used to heat the tube to produce uniform temperature on the cladding circumference (Markiewicz and Erbacher, 1988). This generated a temperature gradient around the cladding. This temperature difference was measured with three thermocouples spot-welded to the outer clad surface. For simulating such a case in OFFBEAT, in addition to the boundary conditions used in the previous case, an azimuthal

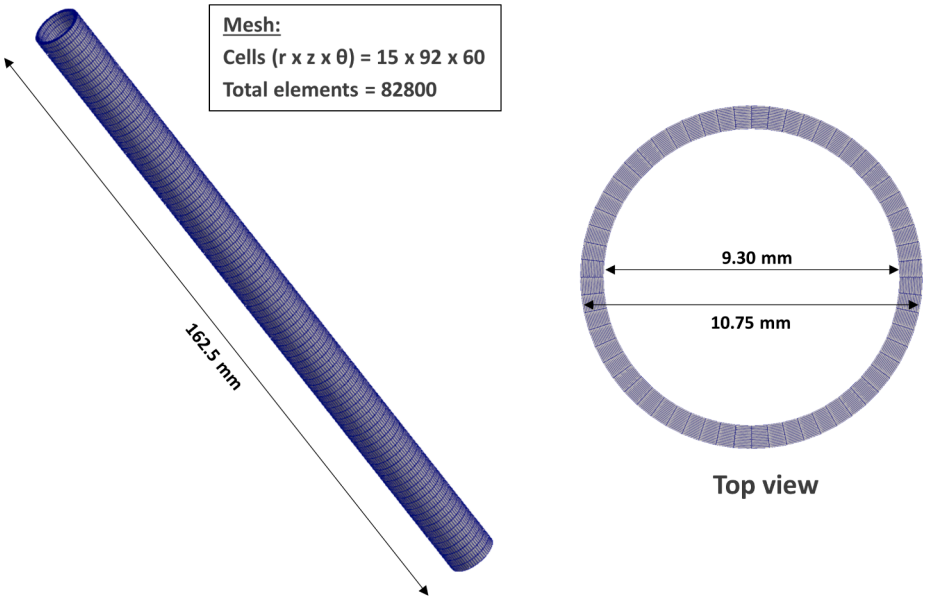

Fig. 9. Geometry and meshing used for the 3D analysis. On the left is the top half length of the cladding tube with its top view on the right.

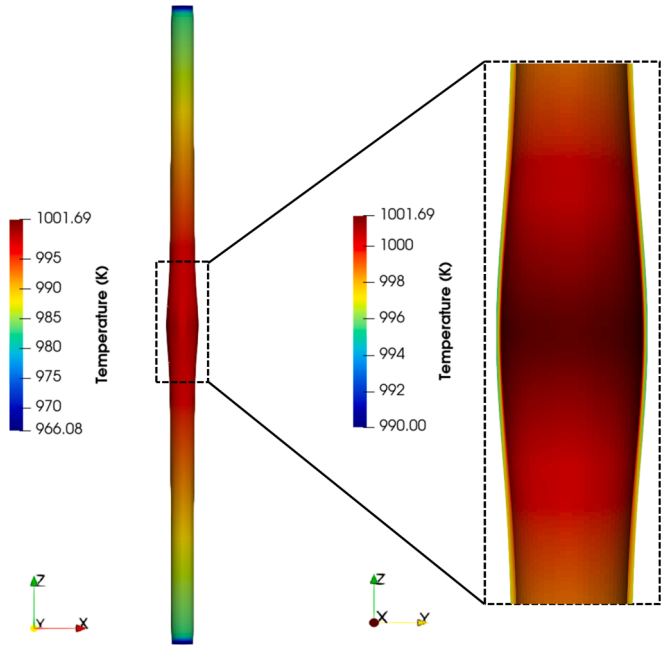

Fig. 10. Contour of cladding tube burst temperature. The view has been sliced in the y-z plane to visualize the effects at the inner surface and zoomed in near the tube mid-plane.

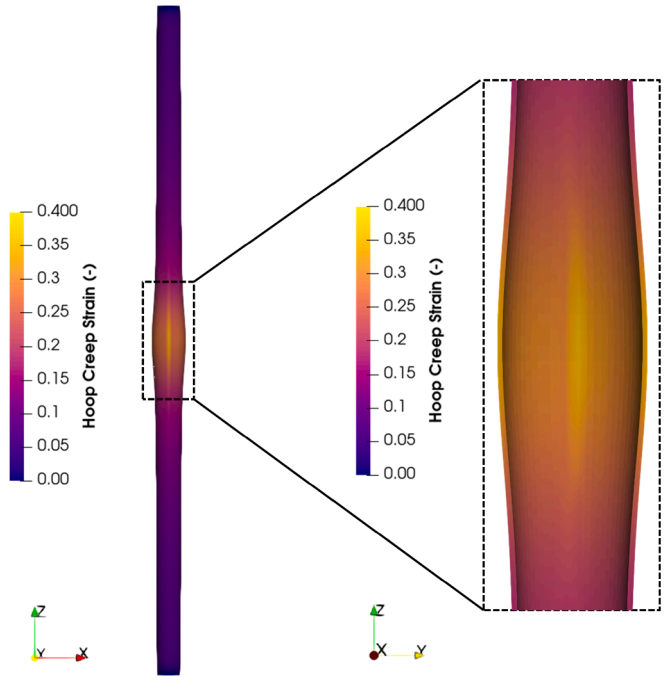

Fig. 11. Contour of cladding tube hoop creep strain. The view has been sliced in the y-z plane to visualize the effects at the inner surface and zoomed in near the tube mid-plane.

temperature gradient was applied. A maximum azimuthal temperature difference of 30 K was assumed, which is the average azimuthal temperature difference from thermocouple measurements in the different tests.

The study was carried out for the case with internal rod pressure of 10 MPa and heating rate of 1 K/s. The simulation was run in parallel on 16 processors and the computation time for this simulation was ≈3 h. The cladding failure occurred at time t = 686.02 s. Similar contours are

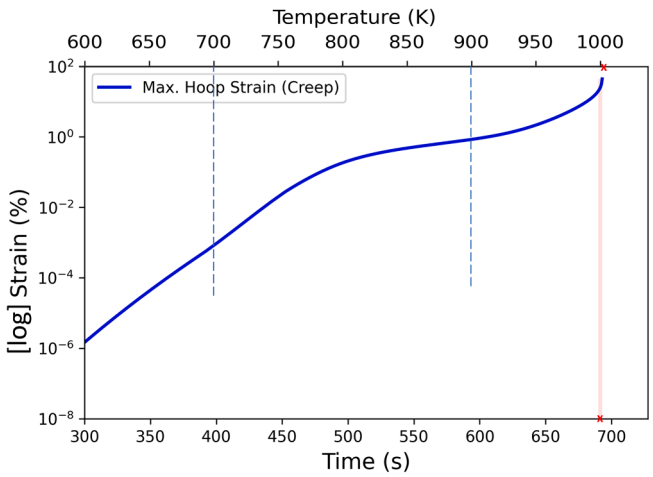

Fig. 12. Time evolution of hoop creep strain for the 3D analysis for case with P = 10 MPa and heating rate = 1 K/s.

Table 3
2D vs 3D results for burst temperature and time of burst.

Burst Temperature (K)		Time of burst (s)	
2D	**3D**	**2D**	**3D**
1002.43	1001.69	693.543	692.787

generated to see the effect of the azimuthal temperature gradient in comparison to the uniform temperature azimuthally in the previous case. Fig. 13 shows the contours for the burst temperature and hoop creep strain in the full-length cladding tube. The localized position where the burst occurred in the cladding is also presented in the figure by rotating the view 90° anti-clockwise.

Unlike the uniform azimuthal temperature case where the ballooning and the deformation was evident only near the mid-plane region, here the cladding can be seen to deform throughout its axial length. This behaviour is explained in the experiments (Markiewicz and Erbacher, 1988) (Erbacher and Leistikow, 1987). Due to its texture and anisotropy, the Zircaloy cladding shows a specific deformation behaviour under uniform temperature conditions with circumferential ballooning accompanied by an axial shortening of the tube. However, under azimuthal temperature gradient conditions, the straining occurs first on the hot side and the cladding experiences an axial shrinkage on this side due to the anisotropy and leads to cladding bowing, forcing it into close contact with the heat source. On the other (colder) side, the cladding deformation is such that it moves away from the heat source (Erbacher and Leistikow, 1987). With this azimuthal temperature gradient, along with the non-uniform deformation and cladding bowing, a higher burst temperature of 1009.43 K was observed. This temperature is ≈9 K higher than the case with uniform azimuthal temperature. This observation is consistent with the BISON results on 3D analysis with an azimuthal temperature gradient, where Pastore et al. (Pastore et al., 2021) observed a burst temperature ≈10 K higher than that in their 2D case.

The non-uniformity and the difference from the uniform temperature case can be observed more precisely in the magnified view near the tube mid-plane in Fig. 14. As is noticed from the figure, the cladding is heated more on one side rather than uniformly. This hot side sees the axial shrinkage of the cladding with the cladding bowing in towards the heater. The hoop creep strain is also higher on this side of the cladding tube and the burst occurs here, with highest hoop creep strain and temperature values. Another thing to notice here is that the burst occurs ≈6 s earlier than in the uniform temperature case, however the

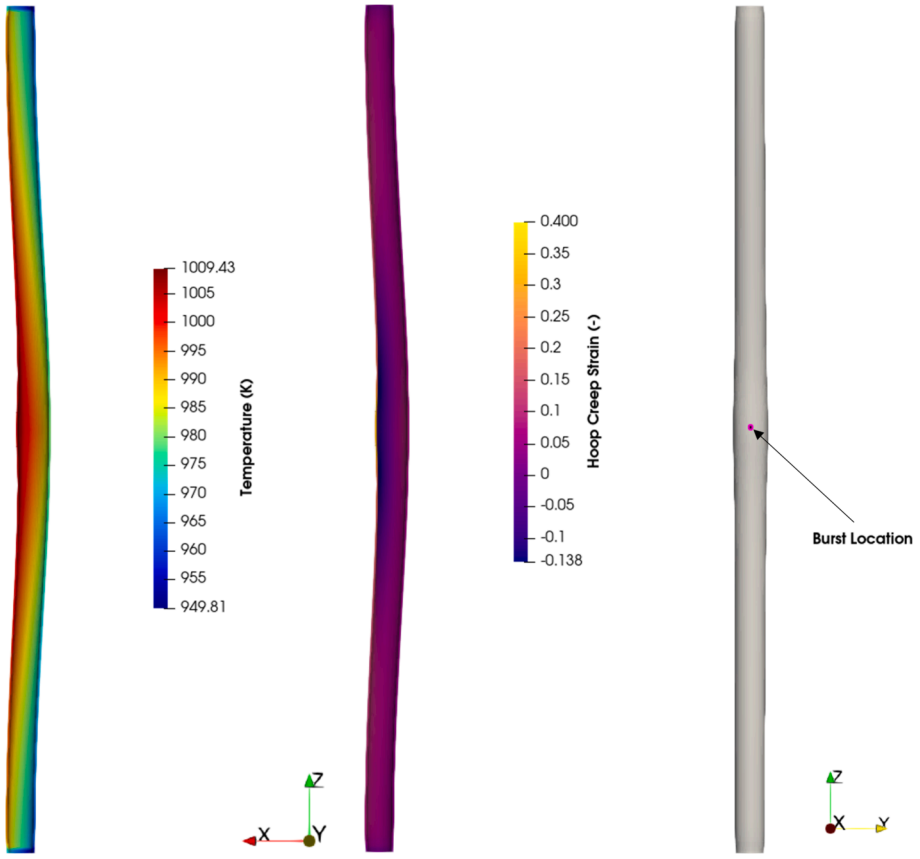

Fig. 13. Contours of cladding tube burst temperature and hoop creep strain for the case with P = 10 MPa and heating rate = 1 K/s with azimuthal temperature gradient of 30 K. Also, the localized position where the burst occurred in the cladding.

temperatures at burst are ≈9 K higher. This suggests that due to the azimuthal temperature gradient, the cladding reaches higher temperatures quickly, leading to early failure.

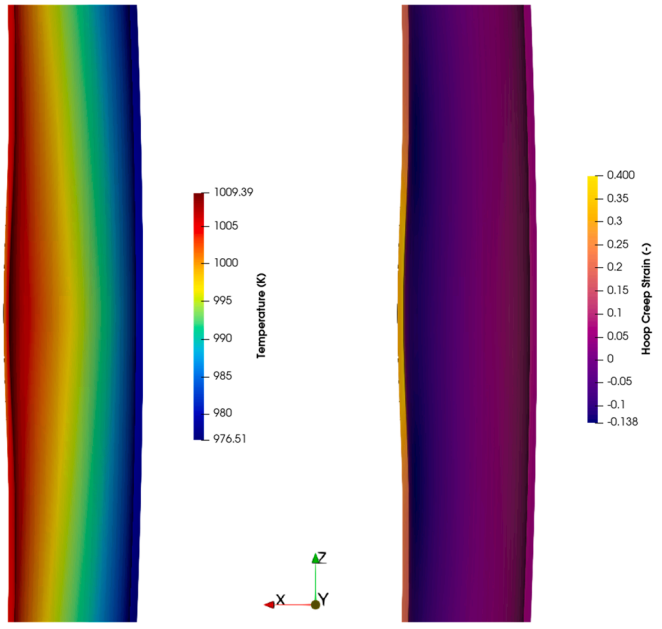

Fig. 14. Temperature and hoop creep strain contours at the time of burst for the case with azimuthal temperature gradient of 30 K. The view has been sliced in the x-z plane to visualize the effects at the inner surface and zoomed in near the tube mid-plane.

5.2.1. Impact of symmetry and zero-displacement boundary conditions

For all the cases analyzed in this paper, a symmetric boundary condition was used on one end of the tube and a fixed value boundary condition on the other. This restrains the tube in the axial direction, causing compressive axial stresses as the tube is heated. Given that the exact mounting of the tubes is not known, this could introduce some unexpected bias in the simulation results. In order to see the impact of these boundary conditions, another simulation of the case with pressure 10 MPa, heating rate 1 K/s and azimuthal temperature gradient of 30 K is carried out. This time the full heating length of the tube (325 mm) is modelled without the symmetry boundary condition. Moreover, a block of cladding to represent the end plug is physically modelled at the bottom end. Fixed pressure boundary conditions with pressure 10 MPa on the end plug inner surface and atmospheric pressure on the end plug outer surface were used to allow axial displacement of the cladding tube.

The contours for the temperature and hoop creep strain at the time of burst in the full-length cladding tube are presented in Fig. 15. A hot side and cold side still exist due to the azimuthal temperature gradient with the highest burst temperature on the hot side reaching 1012.62 K (≈3 K higher than in the fixed value case). The time of burst was found to be 688.99 s (≈2 s higher than the fixed value case). We notice that the bowing of the cladding tube throughout its axial length is reduced significantly in this case. Given that the experiments report noticeable bowing, these results suggest that the experiments were likely conducted using a test rig that limited the axial expansion.

The 3D analysis carried out above provided great insights into the cladding ballooning and burst behaviour in separate-effects tests during LOCA conditions. OFFBEAT was able to obtain results that were in good agreement with the experimental data. The case with azimuthal temperature gradient and resulting bowing showed the importance of 3D codes to access the behaviour which goes unnoticed, or simply cannot be

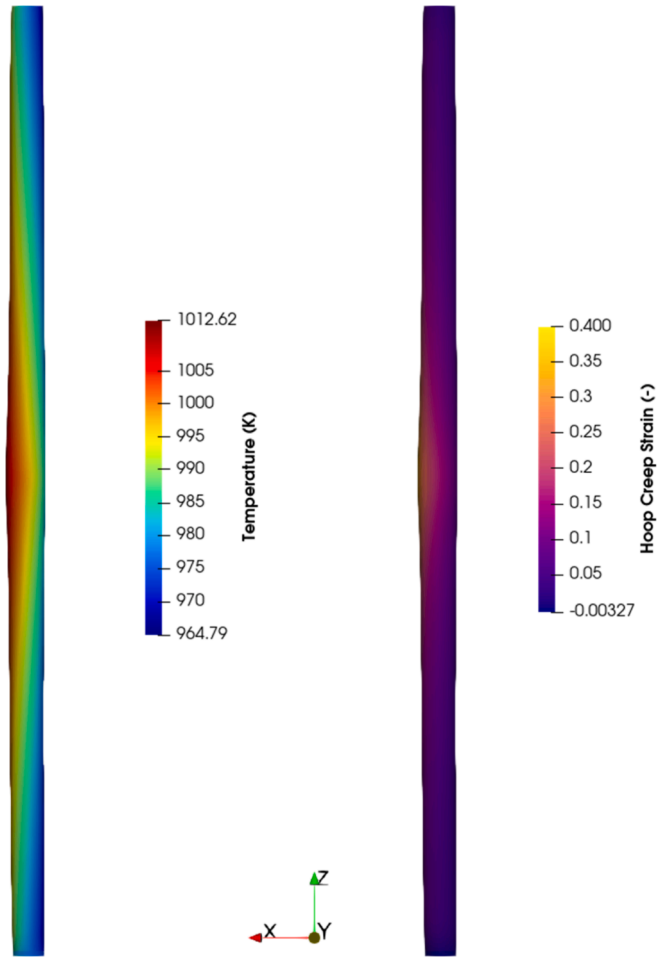

Fig. 15. Contours of cladding tube burst temperature and hoop creep strain for the full tube length for the case with P = 10 MPa and heating rate = 1 K/s with azimuthal temperature gradient of 30 K.

obtained, using 2D analyses.

6. Conclusions

The REBEKA tests for cladding ballooning and burst under LOCA conditions were simulated using OFFBEAT. The REBEKA separate effects tests are temperature transient tests to establish data of cladding ballooning and burst with reference to LOCA conditions. Both 2D and 3D analyses were done to predict the burst temperature as a function of the rod internal pressure. The obtained results were compared with experimental data and were found to be in good agreement at almost all rod internal pressures and heating rates. The results were also compared to analyses available in open literature using the BISON fuel performance code and the results were found to agree well, with even better results at lower values of internal rod pressures. The same validation case with 2D axisymmetric analysis using OFFBEAT was also carried out using Falcon fuel performance code. Mostly the same models were used in the two simulations, however, the creep models adopted for the high temperature regime in Falcon and OFFBEAT are different. The results obtained for the burst temperature versus rod internal pressure were compared and it was found that although similar trends are obtained, Falcon underpredicted the burst temperature values for almost all internal pressure values. Further investigation of the hoop creep strain as a function of temperature showed that the strain values in Falcon remain low in comparison to OFFBEAT, however similar trends for the curve are observed with the two codes. As the burst occurs earlier in Falcon in comparison to the experimental data, this confirms Falcon's usage of a conservative creep model for LOCA.

The 3D results on OFFBEAT faired very well against the results of the 2D analysis. Benefiting from the promising results of the 3D analysis, a study for the effect of azimuthal temperature variation was also carried out. This resulted in non-uniformity of temperature and hoop strain values along the cladding tube length leading to non-uniform deformation and cladding bowing and bending. Similar observations were made in the experiments. The validation study provided great insights into the cladding ballooning and burst behaviour in separate-effects tests during LOCA conditions. OFFBEAT was able to obtain results that were in good agreement with the experimental data. The case with azimuthal temperature gradient showed the importance of 3D codes to access the behaviour which goes unnoticed, or simply cannot be obtained, using 2D analyses. Next step would be to validate OFFBEAT for integral tests on LOCA conditions to further strengthen the confidence in OFFBEAT modelling capabilities for accident conditions. Furthermore, more recent experiments using high-speed cameras and 3D characterization of the final geometry, can provide more detailed data on cladding deformations and strain histories. OFFBEAT validation of such experiments to get more accurate and comparable results can be pursued in the future.

Declaration of competing interest

The authors declare that they have no known competing financial interests or personal relationships that could have appeared to influence the work reported in this paper.

Data availability

The data used is publicly available.

Acknowledgments

The authors acknowledge all the financial support received for this work. This project has received funding from the Euratom research and training programme 2021–2027 through the OperaHPC project under grant agreement 101061453. The work carried out in this paper was also partially funded by the Swiss Federal Nuclear Safety Inspectorate (ENSI) under the JEFFBEAT Project.

References

Ahrens, J., Geveci, B., Law, C., 2005. ParaView: An End-User Tool for Large Data Visualization, Elsevier, ISBN-13: 9780123875822, 2005, .

Berna, G.A., Beyer, C.E., Davis, K.L., Lanning, D.D., 1997. FRAPCON-3: a computer code for the calculation of steady-state, thermal-mechanical behavior of oxide fuel rods for high burnup. US Nuclear Regulatory Commission (NRC) 2. NUREG/CR-6534.

Brunetto, E.L., Scolaro, A., Fiorina, C., Pautz, A., 2023. Extension of the OFFBEAT fuel performance code to finite strains and validation against LOCA experiments. Nucl. Eng. Desig. 406, 112232 https://doi.org/10.1016/j.nucengdes.2023.112232.

Coreform Cubit (Version 2022.11), [Computer software]. Orem, UT: Coreform LLC, https://coreform.com.

Di Marcello, V., Schubert, A., van de Laar, J., Van Uffelen, P., 2014. The TRANSURANUS mechanical model for large strain analysis. Nucl. Eng. Desig. 276, 19–29. https://doi.org/10.1016/j.nucengdes.2014.04.041.

Ek, M., 2005. LOCA testing at Halden; the second experiment IFA-650.2, OECD Halden Reactor Project.

Erbacher, F.J., Neitzel, H.J., Rosinger, H., Schmidt, H., Wiehr, K., 1982. Burst criterion of Zircaloy fuel claddings in a loss-of-coolant accident, Proceedings of the Fifth Conference on Zirconium in the Nuclear Industry, ASTM, pp. 271-283.

Erbacher, F., Leistikow, S., 1987. Zircaloy fuel cladding behavior in a loss-of-coolant accident: a review. Zirconium in the Nuclear Industry: Seventh International Symposium, ASTM STP 939, 451–488.

Gaston, D., Newman, C., Hansen, G., Lebrun-Grandié, D., 2009. MOOSE: a parallel computational framework for coupled systems of nonlinear equations. Nucl. Eng. Desig. 239, 1768–1778. https://doi.org/10.1016/j.nucengdes.2009.05.021.

Geelhood, K.J., Luscher, W.G., Beyer, C.E., Cuta, J.M., 2011. FRAPTRAN 1.4: a computer code for the transient analysis of oxide fuel rod. US Nuclear Regulatory Commission (NRC). NUREG/CR-7023-1.

Geelhood, K.J., Luscher, W.G., Beyer, C.E., 2011. FRAPCON-3.4: integral assessment. US Nuclear Regulatory Commission, Technical Report NUREG-CR-7022 vol. 2.

Hagrman, D.L. Reyman, G.A., 1979. A handbook of materials properties for use in the analysis of light water reactor fuel rod behavior, MATPRO Version 11, in NUREG/CR-0497 (TREE-1280), US Nuclear Regulatory Commission (NRC).

Helfer, T., 2015. Extension of mono-dimensional fuel performance codes to finite strain analysis using a Lagrangian logarithmic strain framework. Nucl. Eng. Desig. 288, 75–81. https://doi.org/10.1016/j.nucengdes.2015.02.010.

Lassmann, K., 1992. TRANSURANUS: a fuel rod analysis code ready for use. J. Nucl. Mater. 188, 285–302. https://doi.org/10.1016/B978-0-444-89571-4.50046-3.

Limbäck, M., Andersson, T., 1996. A Model for analysis of the effect of final annealing on the in-and out-of-reactor creep behavior of zircaloy cladding. ASTM Special Technical Publication 1295, 448–468.

Marelle, V., et al., 2016. New developments in ALCYONE 2.0 fuel performance, in Top Fuel: LWR Fuels with Enhanced Safety and Performance.

Markiewicz, M.E., Erbacher, F., 1988. Experiments on Ballooning in Pressurized and Transiently Heated Zircaloy-4 Tubes, Technical Report KfK 4343, Kernforschungszentrum Karlsruhe, Germany.

Massih, A.R., 2009. Transformation kinetics of zirconium alloys under non-isothermal conditions. J. Nucl. Mater. 384 (3), 330–335. https://doi.org/10.1016/j.jnucmat.2008.11.033.

Pastore, G., Williamson, R.L., Gardner, R.J., Novascone, S.R., Tompkins, J.B., Gamble, K. A., Hales, J.D., 2021. Analysis of fuel rod behavior during loss-of-coolant accidents using the BISON code: Cladding modeling developments and simulation of separate-effects experiments. J. Nucl. Mater. 543, 152537 https://doi.org/10.1016/j.jnucmat.2020.152537.

Perez-Feró, E., Győri, C., Matus, L., Vasáros, L., Hózer, Z., Windberg, P., Maróti, L., Horváth, M., Nagy, I., Pintér-Csordás, A., Novotny, T., 2010. Experimental database of E110 claddings exposed to accident conditions. J. Nucl. Mater. 397 (1–3), 48–54. https://doi.org/10.1016/j.jnucmat.2009.12.005.

Rashid, Y., Dunham, R., Montgomery, R., 2004. Fuel analysis and licensing code: FALCON MOD01. EPRI Report 1011308.

A. Rohatgi, WebPlotDigitizer, Version 4.6, https://automeris.io/WebPlotDigitizer.

Scolaro, A., Clifford, I., Fiorina, C., Pautz, A., 2020. The OFFBEAT multi-dimensional fuel behavior solver. Nucl. Eng. Desig. 358, 110416 https://doi.org/10.1016/j.nucengdes.2019.110416.

Scolaro, A., Fiorina, C., Clifford, I., Brunetto, E., Pautz, A., 2022. Pre-release validation database for the multi-dimensional fuel performance code OFFBEAT. International Conference on Physics of Reactors (PHYSOR) 2914–2923.

Scolaro, A., 2021. Development of a Novel Finite Volume Methodology for Multi-Dimensional Fuel Performance Applications, PhD Thesis. École Polytechnique Fédérale de Lausanne, https://doi.org/10.5075/EPFL-THESIS-8822.

Stuckert, J., Große, M., Rössger, C., Steinbrück, M., Walter, M., 2018. Results of the LOCA reference bundle test QUENCH-L1 with Zircaloy-4 claddings. Technical Report KIT-SR 7651.

Van Uffelen, P., et al., 2008. Verification of the Transuranus fuel performance code-an overview, 7th International Conference on WWER Fuel Performance, Modelling and Experimental Support.

Van Uffelen, P., Konings, R.J.M., Vitanza, C., Tulenko, J., 2010. Analysis of Reactor Fuel Rod Behavior. In: Handbook of Nuclear Engineering, Volume 3. Reactor Analysis, Springer, US, pp. 1519–1627.

Verma, L., Clifford, I., Scolaro, A., Ferroukhi, H., 2024. Extending the validation database of OFFBEAT fuel performance code for LOCA scenarios, in TopFuel2024 Conference.

Wiesenack, W., 2013. Summary of the Halden Reactor Project LOCA test series IFA-650. IFE-OECD Halden Reactor Project, HPR-380.

Williamson, R.L., Pastore, G., Novascone, S.R., Spencer, B.W., Hales, J.D., 2016. Modelling of LOCA Tests with the BISON Fuel Performance Code. No. INL/CON-16-37798, Enlarged Halden Programme Group Meeting.

Williamson, R.L., Hales, J.D., Novascone, S.R., Tonks, M.R., Gaston, D.R., Permann, C.J., Andrs, D., Martineau, R.C., 2012. Multi-dimensional multiphysics simulation of nuclear fuel behavior. J. Nucl. Mater. 432, 149–163. https://doi.org/10.1016/j.jnucmat.2012.01.012.

Williamson, R.L., Gamble, K.A., Perez, D.M., Novascone, S.R., Pastore, G., Gardner, R.J., Hales, J.D., Liu, W., Mai, A., 2016. Validating the BISON fuel performance code to integral LWR experiments. Nucl. Eng. Desig. 301, 232–244. https://doi.org/10.1016/j.nucengdes.2016.02.020.